

# Sub-Terahertz High-Sensitivity High-Resolution Molecular Spectroscopy With a Gyrotron

German Yu. Golubiatnikov, Maksim A. Koshelev , Alexander I. Tsvetkov , Andrei P. Fokin, Mikhail Yu. Glyavin, and Mikhail Yu. Tretyakov

**Abstract**—We explore the possibility of a significant increase in the sensitivity of high-resolution molecular spectroscopy in the sub-THz range by the method of radio-acoustic detection of radiation absorption using the gyrotron as a source of high-power, continuous, frequency-tunable, and highly stable radiation source. We demonstrate that the sensitivity increases in direct proportion to the radiation power until the molecular line saturation is reached. For unsaturated lines corresponding to rotational transitions of methane, a sensitivity of the order of  $\alpha_{\min} \approx 10^{-11} \text{ cm}^{-1}$  is achieved for a power level of about 20 W, which was limited in this work by technical reasons. Examples of spectral line records of other light molecules such as  $\text{SO}_2$ ,  $\text{OCS}$ , and  $\text{CH}_3\text{OH}$  are given. These records permit one to examine the spectral content of gyrotron radiation. The presence of high harmonics without any external frequency multiplier is revealed and evaluated for the first time. Prospects for a further increase in the sensitivity of the method by increasing the radiation power by one or two orders of magnitude are discussed.

**Index Terms**—Gyrotron, high-power radiation, molecular spectroscopy, radio-acoustic detection (RAD), sensitivity, sub-THz range, weakly polar molecules.

## I. INTRODUCTION

A SPECTROMETER with radio-acoustic detection (RAD) and backward-wave oscillators (BWOs) as the sources of radiation was developed at the Institute of Applied Physics of the Russian Academy of Sciences (Nizhny Novgorod, Russia) [1]–[3] and was recognized worldwide [4]–[6]. The spectrometer is used for the study of rotational-vibrational spectra of molecules and precision investigations of individual lines (see the review [7] and references therein). RAD belongs to the class of spectrometers with an opto-acoustic method for detection of electromagnetic radiation [8]–[10], where not a power variation of the radiation transmitted through the sample, but the result of the effect of radiation on matter is recorded. The excitation of molecules at the frequency of the spectral transition and their collisional relaxation lead to heating and expansion of the gas, which is registered by the deflection of a membrane that is the

electrode of a capacitance microphone. The spectrometer output signal  $S$  is directly proportional to the radiation power  $P_{\text{abs}}$  absorbed by the gas

$$S \sim P_{\text{abs}} = P_0 - P = P_0 (1 - e^{-\alpha L})$$

where  $\alpha$  is the absorption coefficient,  $L$  is the optical path length, and  $P_0$  and  $P$  are the radiation power at the input and output of a gas cell, respectively. Under conditions of a low optical depth ( $\alpha L \ll 1$ ) and assuming that  $\alpha$  does not depend on power, the output signal is directly proportional to the studied gas absorption coefficient and to the radiation power fed to the cell,  $S \sim P_0 \alpha L$ . According to the principle of operation, the signal should be observed only within the absorption lines and be absent outside the lines. This is the so-called “zero method,” i.e., the absence of an instrumental baseline against which a signal from the gas absorption line is observed. In real devices, the baseline is present due to the technical reason: the absorption of radiation in the elements of the gas cell (mainly in the windows) leads to their heating and related secondary (nonradiative) heating of the gas.

A characteristic feature of RAD is weak dependence of the spectrometer output signal on the length of the gas cell. The point is that any film used to make a microphone membrane is more rigid than gas at low pressures. In this case, the microphone detects a change in pressure, which is inversely proportional to the volume of the absorption part of the cell. The signal increase related to an increase in the optical depth of the gas is compensated by the same increase in volume. The optimal length of an acoustic cell is estimated as about 10 cm [8] and [10]–[12]. This permits registering intense and weak lines without changing the cell dimensions. In addition, the small length of a cell makes it compact and convenient to use, i.e., for shielding from external magnetic fields when studying the spectra of paramagnetic molecules or for thermal stabilization.

Another feature of the method is the inevitability of a compromise between spectral resolution and sensitivity. The optimal resolution is achieved at pressures where the collisional line broadening is comparable to Doppler. For rotational lines of atmospheric molecules, this occurs at tens of millitorr, and the optimal pressure from the point of view of microphone sensitivity is determined by the rigidity of the membrane, being about 1 torr in real devices (see, e.g., Fig. 4 from [13]).

The versatility of the RAD method allows its use in a wide range of wavelengths without loss of sensitivity, providing a large dynamic range and linearity of the recorded signal. That is

Manuscript received January 15, 2020; revised March 11, 2020; accepted March 27, 2020. Date of publication April 8, 2020; date of current version September 2, 2020. This work was supported by the Russian Science Foundation (Project No. 17-19-01602). (Corresponding author: Maksim A. Koshelev.)

The authors are with the Institute of Applied Physics, Russian Academy of Sciences, 603950 Nizhny Novgorod, Russia (e-mail: glb@ipfran.ru; koma@ipfran.ru; tsvetkov@ipfran.ru; ap.fokin@ipfran.ru; glyavin@ipfran.ru; trt@ipfran.ru).

Color versions of one or more of the figures in this article are available online at <http://ieeexplore.ieee.org>.

Digital Object Identifier 10.1109/TTHZ.2020.2984459

why the spectrometer is intensively used for precision measurements of collisional line shape parameters (see, e.g., [14] and references therein).

The method has a high sensitivity, and with a small length of the cell it detects the absorbed power  $P_{\text{abs}}$  at the level  $10^{-10}$ – $10^{-11}$  W [12], [15]. The absence of a signal outside the absorption line makes it possible to detect weak lines and gas impurities at extremely low relative concentrations of up to  $10^{-13}$  [8]. The use of radiation sources with a higher power improves the spectrometer sensitivity. The weaker the dipole moment of the molecular transition, the greater the improvement which can be achieved (assuming that the technical problem of heating the cell elements by radiation power is resolved). In [16] it was noted that this circumstance, in particular, may open up a possibility for studying forbidden transitions, i.e., rotational spectra of nonpolar molecules. In the optical range, in the presence of high-power laser sources of coherent radiation, the opto-acoustic method has long shown its capabilities and advantages both in nonlinear spectroscopy [17] and when recording weak lines, as well as when microimpurities are detected [18]. For example, in [19], where high-power pulsed lasers of the optical range are used, the sensitivity defined as the minimum detectable absorption is evaluated as  $\alpha_{\text{min}} = 6.8 \cdot 10^{-10} \text{ cm}^{-1}$ .

In the millimeter (mm) and sub-millimeter (sub-mm) wavelength ranges, it is possible to find only a few papers in the field of high-resolution molecular spectroscopy using sources with a high power (more than 1 W). For example, in [20] it was demonstrated that the use of a gyrotron as a radiation source with a radiation power flux of about  $1 \text{ W/cm}^2$  at a wavelength of 2 mm permits observing two-photon rotational transitions of the OCS and  $\text{CHF}_3$  molecules. The estimates made in [21] indicate that the presence of radiation sources with a power flux of more than  $0.1 \text{ W/cm}^2$  would make it possible to obtain a noticeable change in the ratio of spin isomers in the  $^{13}\text{CH}_3\text{F}$  molecule, which is detectable when observing the corresponding rotational lines. As an exotic spectroscopic case the observation of the forbidden ortho-para transition of positronium at 204 GHz using over 20 kW radiation of a gyrotron can be mentioned [22].

The first attempt to use high-power sources of mm radiation for molecular spectroscopy was made in 1974 [23]. An absorption signal corresponding to one of the rotational transitions of the formic acid molecule ( $\text{HCOOH}$ ) was observed using a gyrotron emitting at a frequency of about 34 GHz. The signal was recorded only at the maximum of the absorption line, since the gyrotron did not have a smooth and reproducible tuning of the radiation frequency. This problem explains why the existing gyrotrons were not in demand for spectroscopy in the subsequent decades, although according to the estimates made, the experimental sensitivity was about  $10^{-11} \text{ cm}^{-1}$  for a gyrotron power of  $10^3 \text{ W}$ , which was a record value for that time.

Improvements in the design of gyrotrons manufactured in recent years (see, e.g., the reviews [24], [25] and references therein), made it possible to address again the possibility of their application in the interests of molecular spectroscopy in the mm and sub-mm wavelength ranges. The first trial of molecular spectrum observation with a smoothly tunable but nonstabilized or “free-running” gyrotron is reported in [26].

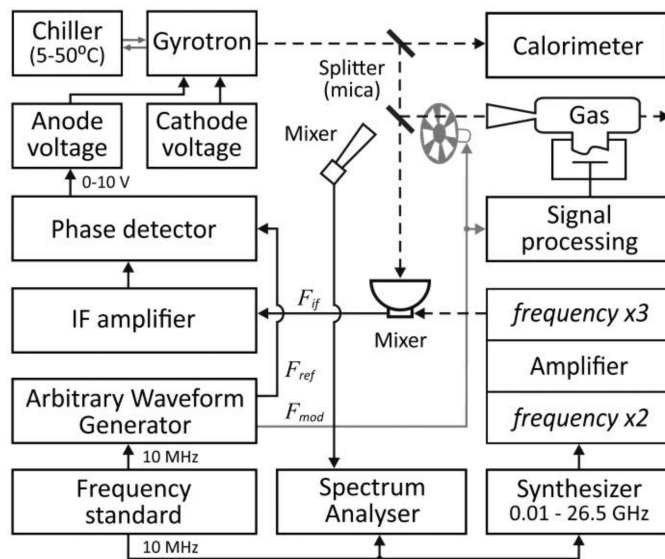


Fig. 1. Block diagram of the RAD spectrometer with a gyrotron having a frequency stabilization system in its version with modulated radiation power.

In this study, we used the same 263-GHz gyrotron operated in the continuous-wave mode. Details on the gyrotron design can be found in [27]. The gyrotron design allows controlling the radiation frequency by changing the voltage at the control anode. This feature was recently used for development and implementation of a phase-locked loop (PLL) system operated by the signal of the reference microwave synthesizer [28]. The PLL system provides precision scanning of the frequency of radiation, as well as its frequency modulation (FM) and phase modulation (PM), which is currently a necessary attribute of most spectroscopic tools. The spectral range available when working with a gyrotron can be significantly extended due to harmonics of the fundamental frequency, which are shown to be an intrinsic property of the powerful gyrotron radiation [29]–[32]. These factors, combined with the conventionally high output power, extend the application range of the gyrotron, making it an attractive tool for high-resolution molecular spectroscopy.

The specifics of using the gyrotron as a highly coherent radiation source in a RAD spectrometer and the new possibilities that have been opened up are demonstrated in this work by recording known rotational lines of the  $\text{SO}_2$ ,  $\text{CH}_3\text{OH}$ , and OCS molecules at both the fundamental and the second, third, and fourth harmonics of the gyrotron radiation frequency. To demonstrate the sensitivity of the method, theoretically predicted low-intensity rotational lines of methane were used. High-power radiation with a high stability provided by the PLL system allowed reaching the absorption sensitivity at a level of  $10^{-11} \text{ cm}^{-1}$  with a clear prospect of further improvement.

## II. EXPERIMENTAL SETUP AND FEATURES OF HIGH-POWER SPECTROSCOPY

A block diagram of the RAD spectrometer with a gyrotron and a system for stabilizing its radiation frequency is shown in Fig. 1. The gas cell, which was similar to that used in [13], [14], and [26], was 2 cm in diameter and 10 cm long.

The acoustic signal was received by a condenser microphone with a Mylar membrane 70 mm in diameter and 0.9  $\mu\text{m}$  thick. The system of capacitance variation recording was made in the form of a high-frequency balanced circuit with the sensitivity  $\Delta C/C \sim 10^{-11}$  [33].

A detailed description of the design features and operating parameters of the gyrotron used as a source of continuous coherent radiation can be found in [27] and [28]. The spectral purity and width of the spectral line of the gyrotron radiation were determined by the PLL system. Measured width of the emission spectrum did not exceed 1 Hz, which corresponded to the maximum resolution of the Keysight N9010A spectrum analyzer being used [28]. Frequency stability was determined by the frequency and time standard SRS FS740, synchronized by a GPS signal and amounted to  $\sim 10^{-13}$  for long-term and  $\sim 10^{-11}$  for short-term relative stability. The range of continuous electronic tuning of the radiation frequency, which was achieved by changing the intermediate frequency in the operating PLL, averaged 20 MHz, reaching 60 MHz for certain parameters of the gyrotron. A wider smooth tuning of the gyrotron frequency in the PLL mode was carried out by a precisely controlled resonator temperature tuning in the same way as in [26]. In this work, we managed to smoothly tune the gyrotron frequency in the PLL mode from 263.1 to 264.0 GHz.

The main part of the gyrotron radiation was directed to a matched load and was measured using a water calorimeter. A small (less than 1/10) part of the radiation, using a quasi-optical divider (a sheet of mica, the thickness of which is much less than the wavelength), was sent to the gas cell of the spectrometer and varied within the range 0.1–20 W.

The main physical constraint on the radiation power and, as a consequence, on the sensitivity of the spectrometers is the maximum power that can be absorbed by the gas in the chosen line, which corresponds to the equalizing of the level populations of the corresponding transition and is characterized by the saturation parameter. If the collisional interaction of molecules can be neglected, the change in the level population difference under the action of continuous resonant radiation has a harmonic form characterized by the Rabi frequency  $\nu_R = d \cdot E/h$  (where  $E$  is the amplitude of the electric field of the radiation,  $h$  is the Planck constant, and  $d$  is the matrix element of the dipole moment of the transition) [34]. The saturation of the spectral transition is reached when the oscillation period of the population difference becomes equal to the collisional relaxation time of the molecules  $\tau = (2\pi\Delta\nu)^{-1}$ , where  $\Delta\nu$  is the collisional half-width of the spectral line of the transition. Herein, the absorption coefficient  $\alpha_0$  at the line center decreases by a factor of 2. The corresponding value of the power flux density  $I_{\text{sat}}$  is called the saturation intensity, which turns out to be proportional to the parameters defining the effect as  $I_{\text{sat}}(\nu) \propto \Delta\nu^2/d^2$  [35].

With allowance for saturation, the absorption coefficient of the collisionally broadened line with the center frequency  $\nu_0$  has the form

$$\alpha_{\text{sat}}(\nu) = \alpha_0 \cdot \frac{\Delta\nu^2}{(\nu - \nu_0)^2 + \Delta\nu^2 \cdot (1 + G_0)}$$

where  $G_0 = (\nu_R/\Delta\nu)^2$  is the saturation parameter. Saturation increases the line width by a factor of  $\sqrt{1 + G_0}$  and decreases absorption in the maximum by a factor of  $(1 + G_0)$ . In terms of spectrometer sensitivity, exceeding the saturating radiation intensity is inexpedient.

The maximum signal will be observed for the radiation source power  $P_{\text{sat}}^{\text{max}} = I_{\text{sat}}(\nu_0) \cdot D \propto h\nu_0 \cdot n^2 \cdot D$  (where  $n$  is the particle density and  $D$  is the cross-sectional area of the interaction of electromagnetic beam with gas), which depends only on the number of absorbing molecules in each particular case [3]. To avoid saturation of the line with increasing power, it is necessary to reduce the power flux density (increase  $D$ ) or increase the gas pressure. Note that the maximum acoustic signal  $S^{\text{max}} \propto \alpha_0 \cdot I_{\text{sat}}(\nu_0)$  at the center of the line of any molecular transition does not depend on the value of  $d$ , because the line intensity is directly proportional to  $d^2$ , while the saturating power is inversely proportional to  $d^2$ . The increase in one is compensated by the same decrease in the other.

The Rabi frequency at a radiation power of 1 kW in a gas cell with a diameter of 2 cm, which is used to record the spectral lines of molecules with matrix elements of the transition dipole moment ranging from 0.1 to 1 D, is from 30 to 300 MHz. Therefore, for recording such lines at pressures of the order of 1 torr that are optimal from the point of view of sensitivity of the used RAD spectrometer cell, which corresponds to a collisional width of several MHz, the power should not exceed 10 W.

Note that a much higher power is needed for a notable saturation of the lines of molecules with a small dipole moment. For example, the asymmetric isotopologue of the carbon dioxide molecule  $^{16}\text{O}^{12}\text{C}^{17}\text{O}$  has a dipole moment of less than  $10^{-5}$  D, and the corresponding saturation power is about 1 GW.

### III. EXPERIMENT AND DATA ANALYSIS

#### A. Spectroscopy of Light Polar Molecules

All measurements were carried out under laboratory conditions at room temperature. The gas pressure in the cell was controlled using a baratron with a manufacturer-declared accuracy of 0.25% of the readings. When choosing gases for research, we proceeded from the need to work with well-studied spectra, which ensures the reliability of the results when demonstrating the capabilities of the method, especially when dealing with harmonics of the radiation. For the first experiments, sulfur dioxide ( $\text{SO}_2$ ) having a dense rotational spectrum, which was studied in, e.g., [36]–[38] was chosen. The lines of this spectrum fall into the range of gyrotron operation, and we used it in the previous studies with an unstabilized gyrotron [26]. The collisional broadening coefficient for most lines in a pure gas is approximately 15 MHz/torr [39]. The pressure of  $\text{SO}_2$  in the cell was chosen in the range 0.02–0.05 torr, then the absorbing gas was diluted with argon as a buffer gas that broadens the  $\text{SO}_2$  lines with a coefficient of about 3 MHz/torr [38] up to a pressure of 0.5 torr, which corresponded to the range of optimal operating pressures of the RAD spectrometer. Thus, the collisional line width was about 2 MHz and the Doppler width was 0.2 MHz.

The RAD method allows using modulation of the radiation power followed by synchronous detection of the absorption

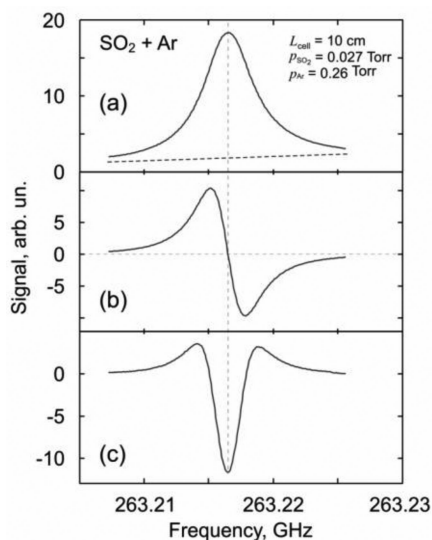


Fig. 2. Examples of the recordings of the  $^{32}\text{SO}_2$  line  $J_{K_a, K_c} = 44_{6,38} \leftarrow 45_{5,41}$ , obtained with a RAD spectrometer and a gyrotron in the PLL mode by different methods of the radiation modulation: (a) modulation of power; (b) and (c) modulation of frequency of the radiation and demodulation of the signal at the (b) first and (c) second harmonics of the modulation frequency, respectively. The dotted line in Fig. 2(a) shows a baseline of the form  $(a \cdot \nu + b)$  resulting from a model function fitting to the experimental recording.

signal at the modulation frequency. This gives certain advantages in the study of the shape of the spectral lines, since it minimizes the number of influencing factors. However, the use of this type of modulation to achieve an ultimate sensitivity (for recording weak signals), and especially with a high radiation power, is not rational, since the spurious signal (baseline) mentioned in the Introduction increases with increasing radiation power. In this case, a weak line is observed against the background of the signal, which can be comparable to or even exceed the amplitude of the line. Moreover, the frequency variations of the spurious signal related to low-Q resonances and radiation interference in the cell and in the waveguide path of the spectrometer can significantly reduce the contrast of recorded lines (see, e.g., Fig. 4 in [26]). To reduce the influence of the baseline when recording a weak signal from the lines, spectroscopy uses the method of the radiation FM followed by demodulation using a synchronous detector. For this purpose, an arbitrary waveform generator (Tektronix AFG3101), which allows modulating the frequency with a given modulation index, was used in the gyrotron PLL as the source of a 35-MHz reference signal for the phase detector. Synchronous detection of the absorption signal was carried out both at the first and second harmonics of the modulation frequency. A 180-Hz frequency modulation was used with a given deviation, the value of which was chosen approximately equal to the collisional width of the observed molecule lines. Examples of experimental recordings of the  $\text{SO}_2$  line  $J_{K_a, K_c} = 44_{6,38} \leftarrow 45_{5,41}$ , obtained with different methods of modulating the radiation signal, are shown in Fig. 2. The baseline determined by optimizing the model profile for the experimental spectrum recorded in the radiation power modulation mode is shown in Fig. 2(a) with a black dotted line.

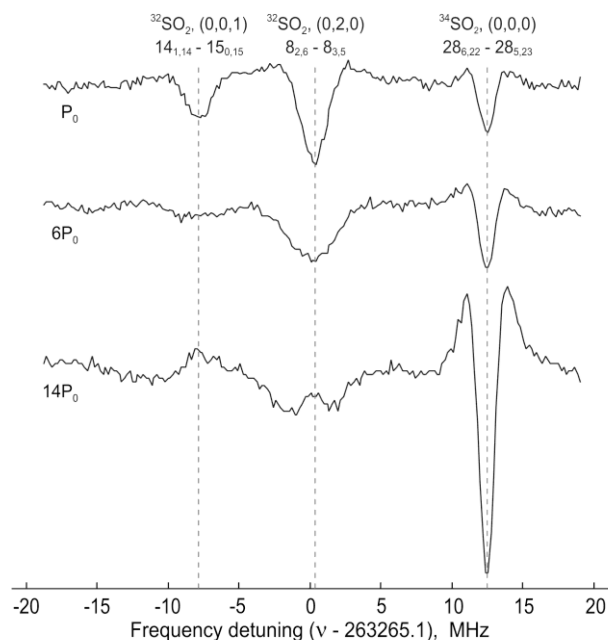


Fig. 3. Spectrum of a  $\text{SO}_2$  mixture with argon (0.027 and 0.26 torr) obtained with a RAD spectrometer and a gyrotron in the PLL mode with modulation of the radiation frequency and synchronous detection of a signal at the second harmonic of the modulation frequency. The factor of radiation power increase is shown in the figure ( $P_0 \sim 0.1$  W).

When interpreting the observed spectra, it is important to take into account that the use of frequency modulation for wide-range recordings leads to the fact that the ratio of amplitudes of the lines [corresponding to the absorption coefficients at the center of the  $\alpha(\nu_0)$  lines] may not correspond to the ratios of their tabular intensities, since the signal amplitude depends on the ratio of the deviation to the line width [40], [41]. When the transition is saturated, absorption decreases at the line center and there occurs a line broadening determined by the value of  $d$ , which can vary significantly for the observed spectral lines of the same molecule. That is, in the mode of wide-range recording of the spectrum with frequency modulation of high-power radiation, it may turn out that the signal from a more intense but broad line will be less than the signal from a weak but narrow line.

A typical example of a change in the observed spectrum with increasing radiation power is shown in Fig. 3. The expected broadening and decrease in peak absorption up to the almost complete disappearance of the line (leftmost and middle lines in Fig. 3) indicate strong saturation of the corresponding transitions. The unusual behavior of the rightmost line becomes clear from the further analysis of the spectra.

Fig. 4 shows a survey recording of the  $\text{SO}_2$  spectrum for a radiation power of the order of 100 mW (upper panel) and the corresponding model spectra, which indicate that some of the observed lines are due to radiation absorption at the strictly doubled and tripled fundamental frequency of the gyrotron radiation. We will call this radiation the corresponding harmonics. It is important not to confuse it neither with the radiation of the operating modes of the gyrotron at the harmonics of the cyclotron frequency, the generation of which is observed for other

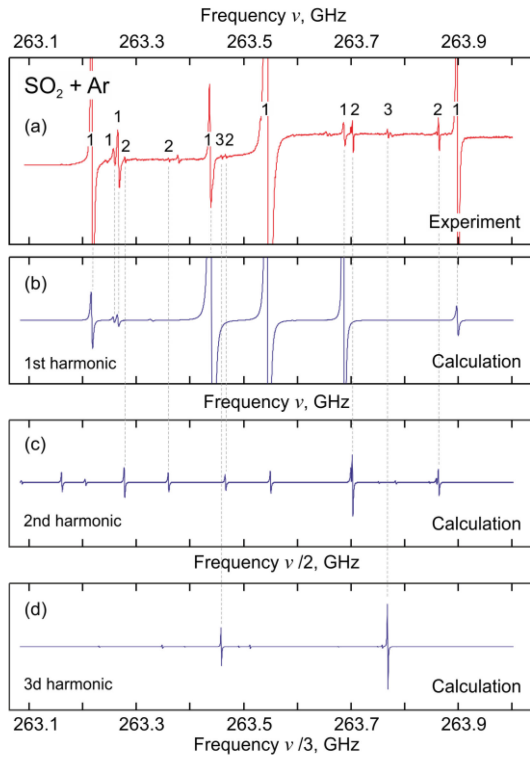


Fig. 4. Survey spectrum of a  $\text{SO}_2$  mixture with argon in the gyrotron tuning range, which was recorded using frequency modulation of the radiation with detection of the absorption signal at the fundamental harmonic of the modulation frequency. The lines are identified as absorption at the fundamental (first), second, and third harmonics of the gyrotron and are marked with corresponding numbers. Bottom panels show the calculated spectra for respective harmonics of the gyrotron radiation.

parameters of the gyrotron [27], nor with the harmonics obtained with external nonlinear elements (frequency multipliers).

To analyze the gyrotron radiation and confirm the presence of harmonics in the gyrotron radiation, we used two dichroic plate filters [42], [43] available in the Lab, which did not pass radiation with frequencies below 300 and 600 GHz. The result of using a 300-GHz high-pass filter (HPF) to analyze the  $\text{SO}_2$  spectrum is shown in Fig. 5.

The  $^{33}\text{SO}_2$  line  $14_{6,8} \leftarrow 15_{5,11}$  at a frequency of 263 686.4 MHz “disappears” in the spectrum, and the other two lines remain virtually unchanged, which indicates their higher frequency nature. This is also evidenced by the fact that the lines corresponding to the second harmonic appears having almost half the width than the lines at the fundamental radiation frequency, since when the frequency of the operating mode is changed by  $\Delta f$ , the frequency of the second harmonic changes synchronously by  $2\Delta f$ . Note that the synchronism of harmonics with the fundamental frequency is also confirmed by the invariance of the phase of the signals from the observed lines during the synchronous detection and use of the PLL system for FM of the radiation.

Assuming the linear dependence of the RAD signal on the radiation power, it is possible to estimate the ratio of the harmonic radiation power to the fundamental radiation power: for unsaturated lines it is equal to the product of the ratio of amplitudes of the observed spectral lines and the inverse ratio of

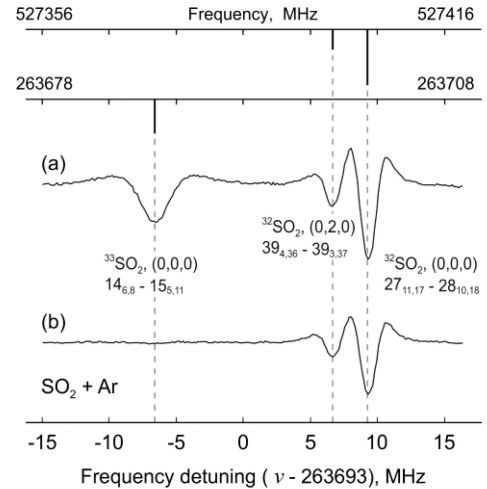


Fig. 5. Spectrum of a  $\text{SO}_2$  mixture with argon (0.035 and 0.475 torr), which was registered (a) without the filter and (b) with an HPF  $f_{\text{cut}} = 300$  GHz (perforated with holes 0.5 mm in diameter) by the RAD method using FM with the absorption signal detected at the second harmonic of the modulation frequency. Vertical thick lines at the upper axes show the tabular (see Table I) positions and intensities of the corresponding transitions.

absorption coefficients at the center of these lines. For example, for the second harmonic

$$\frac{P_0^2}{P_1^2} = \frac{S^2}{S^1} \left( \frac{\alpha_0^2}{\alpha_1^2} \right)^{-1} = \frac{S^2}{S^1} \frac{\Delta\nu^2}{\Delta\nu^1} \frac{I^1}{I^2}$$

where the superscripts 1 and 2 correspond to the lines at the first and second harmonics, and  $I$  is the tabular integrated intensity. An analysis of the observed spectra shows that in our experiments, the radiation power at the second and third harmonics was, respectively, about 1% and 0.1% of the fundamental radiation power. This estimate explains the behavior of the rightmost line in Fig. 2. It corresponds to the transition observed at the second harmonic, the power of which is insufficient for saturation; therefore, the corresponding acoustic signal increases with increasing power, and the line does not broaden.

To confirm the possibility of observing the lines at harmonics, we recorded the lines of OCS carbonyl sulfide (Fig. 6) and  $\text{CH}_3\text{OH}$  methanol (Fig. 7) molecules, the measured frequencies of which also conform well to the tabulated values (Table I) and confirm the correct identification of the lines of the survey spectrum (Fig. 4).

To detect radiation at the fourth harmonic, we chose the  $9_{8,2} \leftarrow 10_{9,1}$  transition of the  $\text{SO}_2$  molecule at a frequency of 1.0559 THz. The calculated absorption coefficient at the center of a collisionally broadened line without saturation for pure  $\text{SO}_2$  is  $\alpha_0 \approx 6.5 \cdot 10^{-2} \text{ cm}^{-1}$ . To reduce the effect of radiation at the fundamental and second harmonics of the gyrotron frequency, we used the 600-GHz HPF. A recording of the line and the fitted model function are shown in Fig. 8. The measured transition frequency and a comparison with known data are given in Table I. The calculated absorption coefficient  $\alpha_0$  at the line center in the studied mixture of  $\text{SO}_2$  with argon is about  $2 \cdot 10^{-2} \text{ cm}^{-1}$ . This allows us to estimate the radiation power at the fourth harmonic frequency as 0.001% of the power of the fundamental harmonic. Note that our estimates of the fraction of radiation at harmonics are rather qualitative. They are only related to the power inside

TABLE I  
TRANSITION FREQUENCIES DETERMINED FROM THE SPECTRA PRESENTED IN FIGS. 2–12 AND THEIR COMPARISON WITH TABULAR VALUES

Figure No.	Molecule	Vibrational state	Rotational state	Measured frequency (MHz)	Intensity (cm/molec)	Tabular value** (MHz)
Fig. 2	$^{32}\text{SO}_2$	(0,0,0)	$44_{6,38} \leftarrow 45_{5,41}$	263216.47	$1.24\text{e-}23$ $1.06\text{e-}23$	263216.4576(43) [45] 263216.459 [39]
Fig. 3	$^{32}\text{SO}_2$	(0,0,1)	$14_{1,14} \leftarrow 15_{0,15}$	263257.29	$1.15\text{e-}2$	263257.353 [44]
	$^{34}\text{SO}_2$	(0,2,0)	$8_{2,6} \leftarrow 8_{3,5}$	263265.33	$1.45\text{e-}2$	263265.148 [44]
	$^{34}\text{SO}_2$	(0,0,0)	$28_{6,22} \leftarrow 28_{5,23}$	526555.10	$9.46\text{e-}2$	526555.0731(127) [45]
Fig. 5	$^{33}\text{SO}_2$	(0,0,0)	$14_{6,8} \leftarrow 15_{5,11}$	263686.40	$1.43\text{e-}23^*$	263686.466* [45]
	$^{32}\text{SO}_2$	(0,2,0)	$39_{4,36} \leftarrow 39_{3,37}$	527399.30	$3.38\text{e-}23$	527399.285(19) [45]
	$^{32}\text{SO}_2$	(0,0,0)	$27_{11,17} \leftarrow 27_{10,18}$	527404.48	$9.35\text{e-}23$	527404.477(8) [45]
Fig. 6	OCS	(0,0,0)	$65 \leftarrow 64$	789163.68	$7.37\text{e-}2$ $5.58\text{e-}2$	789163.8420(25) [45] 789163.7346(13) [46]
Fig. 7	CH <sub>3</sub> OH	gr.	$19_3 \leftarrow 19_2$	526949.96	$2.72\text{e-}22$	526949.841(15) [45]
			$11_1 \leftarrow 10_1$	527053.46	$3.45\text{e-}22$	527053.489(6) [45]
			$15_3 \leftarrow 15_2$	527171.26	$3.72\text{e-}22$	527171.462(14) [45]
Fig. 8	$^{32}\text{SO}_2$	(0,0,0)	$9_{8,2} \leftarrow 10_{9,1}$	1055976.29	$4.5\text{e-}21$ $4.0\text{e-}21$	1055976.2927(72) [45] 1055976.30 [39]
Fig. 9	$^{32}\text{SO}_2$	(0,0,1)	$25_{1,24} \leftarrow 24_{4,21}$	263151.50	$1.3\text{e-}26$	263151.527 [44]
	$^{34}\text{SO}_2$	(0,0,0)	$64_{11,53} \leftarrow 65_{10,56}$	263161.63	$4.5\text{e-}25$	263161.6396(297) [45]
	$^{33}\text{SO}_2$	(0,0,0)	$21_{10,12} \leftarrow 22_{9,13}$		$2.8\text{e-}23^*$	526306.949(18)* [45]
	$^{34}\text{SO}_2$	(0,0,0)	$35_{6,30} \leftarrow 35_{5,31}$		$6.2\text{e-}22$	526321.8127(164) [45]
Fig. 10	$^{12}\text{CH}_4$	00011	$7_2 \leftarrow 6_4$	263767.945	$1.25\text{e-}2$	263768.077 [39]
Fig. 12	$^{12}\text{CH}_3\text{D}$	00001	$8_2 \leftarrow 8_3$	262822.959	$7.89\text{e-}30$	262822.960 [48]

\*Determined as a mean value of hyperfine structure components

\*\*Data from HITRAN are at 296 K, from JPL at 300 K, from [44] at 293 K.

Typical error of determining the frequencies of studied transitions is 10–50 kHz.

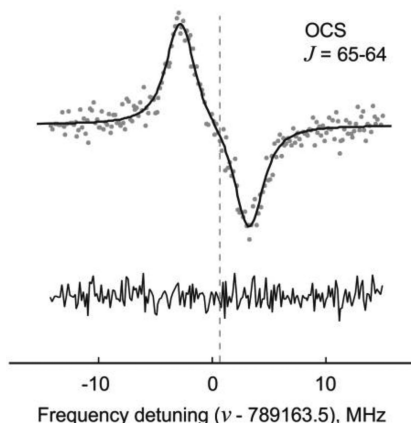


Fig. 6. Recording of the OCS line  $J = 65 \leftarrow 64$  (dots) at the third harmonic of the gyrotron frequency with a 600-GHz HPF (perforated with holes 0.3 mm in diameter). The result of optimizing the model profile based on the Voigt profile to fit the experimental spectrum is shown by a solid line. The difference between the experimental and model profiles is shown at the bottom. The vertical dashed line shows the tabular position of the transition.

the gas cell and do not take into account neither the transmittance of the filters we used nor the difference in the power transfer coefficients from the gyrotron. The latter difference is due to the frequency dependence of the reflection coefficient of the power divider we used and to the different absorption of radiation by atmospheric air in a long (2.5-m) waveguide.

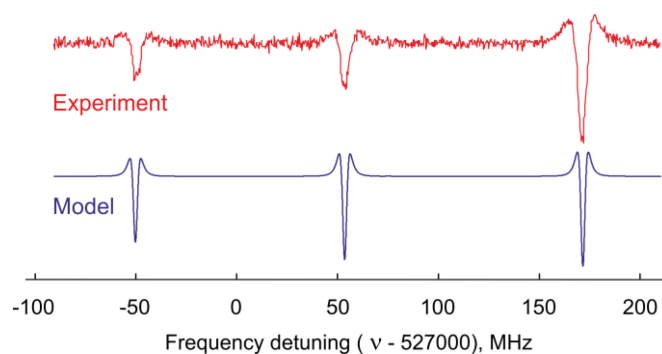


Fig. 7. Experimental spectra of methanol CH<sub>3</sub>OH (red curve) recorded at room temperature using RAD spectrometer with a frequency-stabilized gyrotron at the second harmonic (radiation at the first harmonic was cutoff by a 300-GHz HPF); methanol pressure in the cell was 0.16 torr. Blue curve is model spectrum which was obtained using JPL frequencies and intensities [45], HITRAN self-broadening coefficient  $0.4 \text{ cm}^{-1} \text{ atm}^{-1}$  [39] and experimental conditions (pressure, temperature, and frequency deviation).

Synchronous generation of radiation harmonics in gyrotrons was discussed in experimental [29], [30] and theoretical [31], [32] papers and is apparently a typical phenomenon associated with parametric radiation generation. However, harmonics above the second were not experimentally observed previously by anyone. This is most likely due to difficulties in detecting “weak” harmonics against the background of a strong fundamental frequency signal using standard methods, i.e., signal heterodyning, i.e., transferring the frequency to the low-frequency

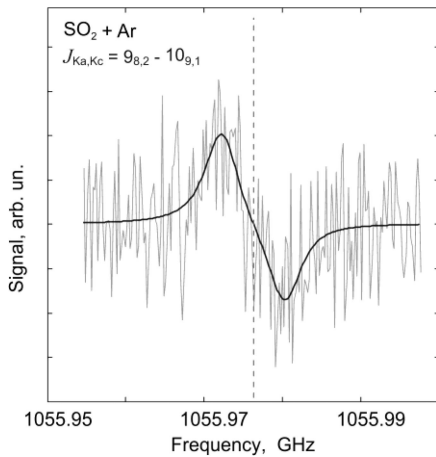


Fig. 8. Recording of the  $\text{SO}_2$  line  $J_{K_a,K_c} = 9_{8,2} \leftarrow 10_{9,1}$  in a  $\text{SO}_2$  mixture with argon (0.035 and 0.465 torr) at the fourth harmonic of the gyrotron frequency with a 600-GHz HPF (gray broken curve). The result of fitting the model profile on the basis of the Voigt profile to the experimental spectrum is shown by a solid line. The vertical dotted line shows the tabular position of the line.

range and studying it using a spectrum analyzer. In our work, it was demonstrated that recording the spectrum of a known gas by the RAD method permits one to uniquely determine the spectral composition of the radiation employed. Thus, a RAD spectrometer cell filled with a gas and having a well-known and fairly dense spectrum can be used as an analyzer of the coherent radiation spectrum of high-power sources. Previously, this opportunity was used for the analysis of the BWO radiation spectrum [47].

The increase in the sensitivity of the RAD cell with increasing radiation power is demonstrated by recording a part of the spectrum of  $\text{SO}_2$  using a BWO and a gyrotron (Fig. 9).

In both experiments, we used a mixture of  $\text{SO}_2$  (with natural abundance of isotopologues) with argon (1:14) at total pressure of 0.5 torr. The synchronous detection of the absorption signal at a double modulation frequency was employed. The signal accumulation time at each frequency point was 0.6 s. The BWO radiation power was approximately 5 mW and the gyrotron power increased from recording to recording. The frequency range under consideration contains the line of a purely rotational transition  $25_{1,24} \leftarrow 24_{4,21}$  of the  $^{32}\text{SO}_2$  molecule in the first excited asymmetric stretching vibrational state ( $\nu_0 = 263\ 151.5$  MHz,  $d \sim 0.12$  D) and the line  $64_{11,53} \leftarrow 65_{10,56}$  of the  $^{34}\text{SO}_2$  isotopologue ( $\nu_0 = 263\ 161.63$  MHz,  $d \sim 0.45$  D). The line  $64_{11,53} \leftarrow 65_{10,56}$  becomes saturated at 0.1 W, and the further increase in power does not lead to an increase in its amplitude. Moreover, this line can overlap on the spectrum recording with the  $35_{6,30} \leftarrow 35_{5,31}$  line of the  $^{34}\text{SO}_2$  molecule ( $\nu_0 = 526\ 321.87$  MHz,  $\nu_0/2 = 263\ 160.93$  MHz) observed at the second harmonic of the gyrotron radiation (Fig. 4(c)). The signals from the lines at the first and second harmonics become comparable with each other when the radiation power is more than 0.5 W, which makes their quantitative analysis virtually impossible. The  $25_{1,24} \leftarrow 24_{4,21}$  line has a significantly smaller matrix element of the transition dipole moment. The signal from

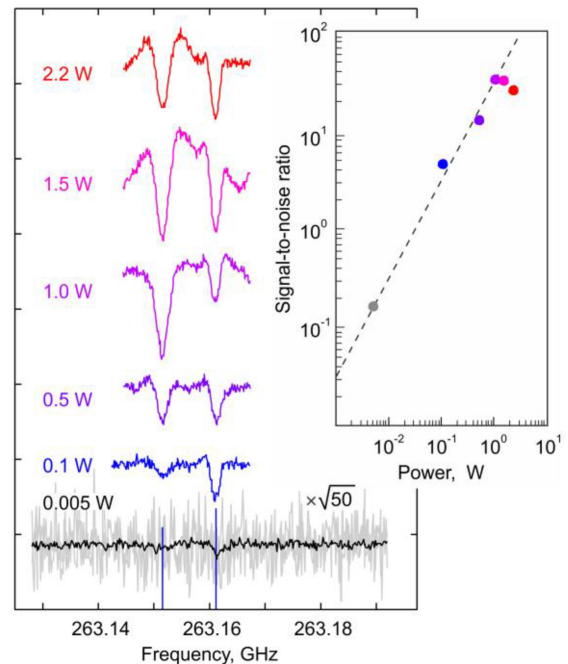


Fig. 9. Recordings of the  $\text{SO}_2$  (a mixture with argon in 1:14 proportion at a pressure of 0.5 torr) spectrum using a radio-acoustic cell for different radiation powers, spaced apart on a vertical scale for clarity. The gray spectrum shows a typical recording with a single range scan obtained using a BWO and the black spectrum is the result of averaging of 50 such recordings. The spectra obtained using a BWO (gray and black) are increased in amplitude by  $\sqrt{50}$  times for easy comparison with other traces. The single scan recordings obtained with a gyrotron for different radiation powers are shown on top. Vertical lines are tabular positions and relative intensities of the lines. The inset shows the  $S/N$  for the low-frequency line in the spectra as a function of the radiation power. The dashed line shows a fitted straight line passing through the origin of coordinates. The colors of dots correspond to the colors of spectra on the left.

it increases with increasing power up to 1 W. The further increase in power leads to saturation of the transition and a decrease in the signal from the line. In the spectra obtained using a BWO, the amplitudes of both lines are several times lower than the noise level. The lines can only be detected by repeating recordings many times and averaging them. The result of averaging of 50 recordings is shown in Fig. 9. The signal-to-noise ratio ( $S/N$ ) on the line was defined as a difference between the minimum and maximum of the model function fitted to the observed line, divided by the standard deviation of noise in the corresponding spectrum recording. An analysis of the obtained spectra confirms that the  $S/N$  on the observed line, and therefore the sensitivity of the spectrometer, increase in direct proportion to power till the transition saturation.

This preliminary experiment gives grounds for confidence that an increase in the power of the radiation by many orders of magnitude compared to conventional spectroscopic sources will make it possible to achieve an outstanding sensitivity of the RAD method in the study of lines with a transition dipole moment of 0.01 D or less.

### B. Spectroscopy of Weakly Polar Molecules

The line of a purely rotational transition of the  $\text{CH}_4$  molecule  $J_K = 7_2 \leftarrow 6_4$  with symmetry  $F_1$  in the  $\nu_4 + \nu_5$  vibrational

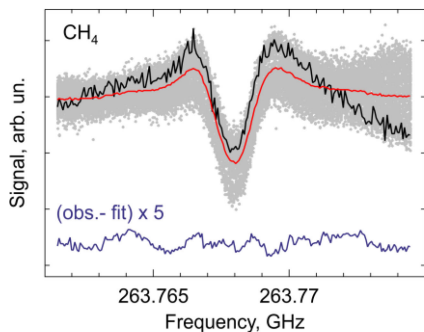


Fig. 10. Results of observation of the  $\text{CH}_4$  line  $J_K = 7_2 \leftarrow 6_4$  in the vibrational state  $\nu_4 + \nu_5$  with a peak absorption of about  $10^{-9} \text{ cm}^{-1}$ . The black line is a single step-by-step recording of the spectrum, the gray dots correspond to all amplitude samples obtained as a result of 104 such recordings, and the red line is the result of averaging of all the samples. The blue line is the residue of fitting the model function to the averaged spectrum.

state excited by collisions and having an integrated intensity of  $1.249 \cdot 10^{-29} \text{ cm/mol}$  [39] was chosen for the trial. The dipole moment of the transition is due to the centrifugal distortion of the symmetrical structure of the molecule. For the experiment, we used a gas sample with a 99% content of  $\text{CH}_4$ . The spectrum was recorded for a pressure of 0.26 torr. The radiation power was increased up to  $\sim 15 \text{ W}$ . The further increase led to overheating of the gas cell windows made of high-density polyethylene and not designed for radiation intensity so high in ordinary spectroscopy. The heating of the windows of the acoustic cell led to an increase in the spurious signal mentioned above, and the turbulent air flows arising in front of the input window of the cell due to heat emission impaired the stability of experimental conditions. It appeared most optimal for recording spectra under such conditions to decrease the synchronous detection time constant to 0.1 s and increase the number of averaged spectra. A single (back-and-forth) step-by-step recording of the spectrum at 200 points in the vicinity of the line center took a little less than 1 min. A total of 104 such recordings were obtained. The signal was detected at a double modulation frequency. The results of two-hour recording of the spectrum and its preliminary analysis are presented in Fig. 10. The model function used to analyze the line was built on the basis of the Lorentz profile. Hardware effects, including the dependence of the average radiation power on frequency and the presence of a baseline, were approximated by polynomials of the first and second order, respectively. The residue of fitting the model function to the averaged spectrum is shown in the lower part of Fig. 10 with fivefold magnification.

The achieved absorption sensitivity of the spectrometer or the minimum detectable signal  $\alpha_{\min}$  was determined by dividing the absorption coefficient  $\alpha_0$  at the line center by the  $S/N$  on the spectrum recording. For the estimates, we used tabular data on the integrated intensity  $I$  normalized to the concentration of absorbing molecules and the collisional broadening coefficient  $\gamma$  [39], as well as the fact that the integrated intensity of the Lorentz profile is proportional to the product of its width and amplitude [35]

$$\alpha_{\min} = \frac{I}{\pi \gamma k T (S/N)}$$

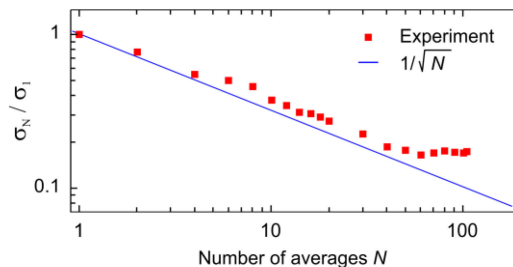


Fig. 11. Normalized standard deviation  $\sigma_N/\sigma_1$  of the fit residual for the  $J_K = 7_2 - 6_4$  line of  $\text{CH}_4$  obtained by fitting the result of averaging of  $N$  repeated experimental records of the spectrum.

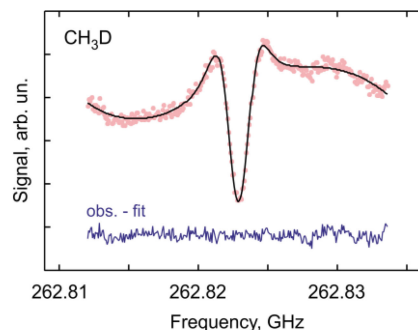


Fig. 12. Result of observation of the  $\text{CH}_3\text{D}$  line ( $8_2 \leftarrow 8_3$ , E,  $\nu_5$ ) with the peak absorption of  $6 \cdot 10^{-10} \text{ cm}^{-1}$ . The dots show averaging of 40 single recordings (back-and-forth) of the spectrum. The black line is a fitted model function. The blue line is a residue.

where  $k$  is the Boltzmann constant and  $T$  is the gas temperature.

The  $S/N$  on the methane line shown in Fig. 10 is about 80, while  $\alpha_{\min} = 1.3 \cdot 10^{-11} \text{ cm}^{-1}$  or taking into account the integration time  $\alpha_{\min} = 8.4 \cdot 10^{-10} \text{ cm}^{-1} \text{ Hz}^{-0.5}$ .

The multiple line records from this experiment (Fig. 10) were used for determining the total signal integration time after which the averaging process becomes inefficient or even counterproductive. The corresponding Allan variance plot (Fig. 11) demonstrates decreasing of the standard deviation  $\sigma_N$  of the fit residual as  $N^{-0.5}$  up to  $N = 60$ , which can be considered an optimal number of single records of the line in the conditions of our experiment.

To verify the achieved sensitivity, we recorded another low-intensity line corresponding to the rotational transition  $J_K = 8_2 \leftarrow 8_3$  of the monodeuterated methane isotopologue in the excited vibrational state  $\nu_5$  with an integrated intensity of  $7.89 \cdot 10^{-30} \text{ cm/molec}$  (parameters of the line were determined within the framework of our recent spectroscopic study [48]). The  $\text{CH}_3\text{D}$  content in the sample was approximately 90%. The dipole moment of the molecule is  $\sim 6 \cdot 10^{-3} \text{ D}$  with a significant rotational dependence [49]. The spectrum was recorded for a pressure of 0.3 torr following the same procedure as in the previous experiment, but in a wider frequency range. The result of averaging of 40 single recordings is shown in Fig. 12. To adequately describe the observed signal with a model function, we had to increase the degree of the polynomial responsible for the frequency dependence of the baseline to the fourth. The fitting result and the residue are shown in Fig. 12.

The  $S/N$  in the spectrum recording is about 30. To evaluate the sensitivity, we used the data on collisional broadening of the  $\text{CH}_3\text{D}$  ro-vibrational transitions with the same rotational quantum numbers from [50]. Taking into account the 90% concentration of absorbing molecules in the gas, the minimum detectable absorption was  $1.6 \cdot 10^{-11} \text{ cm}^{-1}$  or  $6.5 \cdot 10^{-10} \text{ cm}^{-1} \text{ Hz}^{-0.5}$ , which fully confirmed the previous result.

Note that both methane lines presented here were not previously observed in experiments. Their frequencies and intensities were predicted in [39], [48], and [51]. Despite the fact that the error of the line frequencies determination is estimated by HITRAN experts as 30–300 MHz, the observed positions of the  $\text{CH}_4$  and  $\text{CH}_3\text{D}$  lines differ from the predictions by  $-0.13(3)$  and  $-0.001(20)$  MHz, respectively, which indicates that the error estimate in HITRAN is conservative. The line intensity uncertainty is estimated in HITRAN as  $\geq 20\%$ .

For comparison with the sensitivity of other methods, we refer a reader to two recent studies of the rotational spectrum of  $\text{CH}_4$  [52], [53]. The first paper presents the first observations of the  $\text{CH}_4$  spectrum using the SOLEIL synchrotron facility and a high resolution Fourier-transform spectrometer equipped with a 150-m path-length gas cell. Lines with integrated intensity greater than  $2 \cdot 10^{-26} \text{ cm/molec}$  were observed after about 30 h of integration time. The photomixing CW-THz spectrometer coupled to the 20-m path-length cell was used in the second work. The  $R(7)$  line with integrated intensity of  $2.94 \cdot 10^{-25} \text{ cm/molec}$  was recorded with  $S/N = 8$  after a signal accumulation period of 4 h.

#### IV. CONCLUSION

The possibilities of increasing the sensitivity of radioacoustic molecular spectroscopy by using a high-power gyrotron source operating in the sub-THz frequency range have experimentally been explored as follows.

- 1) The possibility of detecting molecular spectral lines with an intensity of about  $10^{-30} \text{ cm/molec}$  for a line recording time of about 1 min is shown.
- 2) The system of precision monitoring and digital control of the gyrotron radiation frequency based on the PLL system combined with high stability of the radiation power, permitted high-precision studies of high-resolution molecular spectra with the analysis of the shape of the observed lines and determination of their spectroscopic parameters, including long-term (a few hours) accumulation of the absorption signal. Signal accumulation for about 1 h made it possible to achieve an absorption sensitivity of about  $10^{-11} \text{ cm}^{-1}$  or better than  $10^{-9} \text{ cm}^{-1} \text{ Hz}^{-0.5}$ .
- 3) Further increasing the absorption detection sensitivity by increasing the radiation power was limited by the technical reason, namely, overheating of the windows used in the RAD cell. The maximum power was less than 20 W, which is several orders of magnitude higher than the radiation power of the mm-sub-mm wavelength sources that are conventional for spectroscopy and 1 or 2 orders of magnitude lower than the maximum power for the gyrotron we used. The possibility of the further sensitivity increase will

be verified after low-loss diamond windows for the gas cell are manufactured. Radiation loss in diamond is about two orders of magnitude less than in high density polyethylene (HDPE) which was used for the current windows.

- 4) The possibility of spectroscopy at harmonics of the gyrotron has been demonstrated. Harmonics are an intrinsic property of the gyrotron radiation; they are multiple and synchronous with the fundamental radiation. The spectral analysis of gyrotron radiation performed in this work confirmed the possibility of using the RAD method to evaluate the frequency and power characteristics of radiation sources.

The most important result seems to be the potential possibility of further increasing the sensitivity of the spectrometer by increasing the power of the radiation. This can be implemented after manufacturing the gas cell windows from artificial diamond. The sensitivity increase opens up a possibility for detecting weak, and therefore poorly studied, molecular lines corresponding to transitions with very small matrix elements of the dipole moment. One example of such lines is transitions of paramagnetic molecules occurring due to the magnetic dipole moment. The latter is usually equal to 1 Bohr magneton, which is equivalent to an electric dipole moment of about 0.01 D. As a typical representative, one can point to the rotational spectra of an oxygen molecule in excited vibrational states, which were never studied in the sub-mm range due to the lack of sensitivity of the spectrometers. Note that the rotational-vibrational spectrum of oxygen is not observed in the IR range because of the absence of the derivative of the dipole moment with respect to the bond length between atoms. Another object of research can be poorly explored rotational spectra of isotopologues of symmetric diatomic and linear molecules, such as  $^{14}\text{N}^{15}\text{N}$ ,  $^{16}\text{O}^{17}\text{O}$ ,  $^{16}\text{O}^{12}\text{C}^{17}\text{O}$ , etc., whose individual lines were studied only in the cm and mm wavelength range [54]–[57]. Another class of objects relates to molecules of the symmetric and spherical top type. These are analogues of the  $\text{CH}_4$  line observed in this work, which are forbidden in the rigid top approximation. A small dipole moment occurs during the rotation of molecules due to distortion of its structure by centrifugal forces. Studies of the quadrupole transitions of nonpolar molecules, which are forbidden in the electric dipole approximation, as well as transitions between spin isomers of the molecules, which are still more forbidden, i.e., transitions between para and ortho states, are most interesting for fundamental spectroscopy (see, e.g., [21], [58]). The opening field of the spectroscopy of nonpolar molecules in a strong electromagnetic field is even more exciting. In contrast to conventional spectroscopy, which usually does not disturb either the state of the gas or the molecular structure, it might be possible to study the effects associated with molecular polarizability (field induced dipole moment) [35]. For polar molecules, the almost unlimited (in terms of conventional spectroscopic standards) power of highly coherent radiation permits one to consider the possibility of multiphoton spectroscopy (see, e.g., [20]).

Cumulative result of this work allows us to talk of a RAD spectrometer with a gyrotron as a radiation source and a PLL-based frequency control system as of a promising terahertz

spectrometer (GyroRAD) for studying the weakest molecular lines corresponding to a small dipole moment of molecular transitions and determining their quantitative characteristics.

#### ACKNOWLEDGMENT

The authors are grateful to Prof. A.F. Krupnov for fruitful discussions and valuable comments on the manuscript.

#### REFERENCES

- [1] A. F. Krupnov, L. I. Gershtein, V. G. Shustrov, and S. P. Belov, "A radiospectroscope with acoustic display for the millimeter and submillimeter ranges," *Izv. VUZov. Radiofizika*, vol. 13, no. 9, pp. 1403–1405, 1970.
- [2] A. F. Krupnov and A. V. Burenin, *New Methods in Submillimeter Microwave Spectroscopy*, in *Molecular Spectroscopy: Modern Research*, vol. 2, K. N. Rao, Ed., New York, NY, USA: Academic, 1976.
- [3] A. F. Krupnov, "Modern submillimeter microwave scanning spectroscopy," in *Modern Aspects of Microwave Spectroscopy*, G. W. Chantry, Ed., London, U.K.: Academic, 1979, pp. 217–256.
- [4] E. B. Wilson, "Molecular spectroscopy," *Annu. Rev. Phys. Chemistry*, vol. 30, no. 1, pp. 1–28, 1979.
- [5] W. Gordy, "Early events and some later developments in microwave spectroscopy," *J. Mol. Struct.*, vol. 97, pp. 17–32, 1983, doi: [10.1016/0022-2860\(83\)90172-2](https://doi.org/10.1016/0022-2860(83)90172-2).
- [6] W. Gordy and R. L. Cook, *Microwave Molecular Spectra* (Techniques of Chemistry), vol. 18, 3rd ed. New York, NY, USA: Wiley, 1984, p. 929.
- [7] A. F. Krupnov *et al.*, "Accurate broadband rotational BWO-based spectroscopy," *J. Mol. Spectrosc.*, vol. 280, pp. 110–118, 2012.
- [8] L. B. Kreuzer, "Ultralow gas concentration infrared absorption spectroscopy," *J. Appl. Phys.*, vol. 42, no. 7, 1971, Art. no. 2934.
- [9] V. S. Letokhov, "Problems of laser spectroscopy," *Uspekhi Fizicheskikh Nauk*, vol. 118, pp. 199–249, 1976.
- [10] V. P. Zharov and V. S. Letokhov, *Laser Optoacoustic Spectroscopy*. Berlin, Germany: Springer-Verlag, 1986.
- [11] S. P. Belov, A. V. Burenin, L. I. Gershtein, V. V. Korolikhin, and A. F. Krupnov, "Broad-banded millimeter and submillimeter microwave spectroscopy of gases with high sensitivity," *Optika i Spektroskopiya*, vol. 35, no. 2, pp. 295–302, 1973.
- [12] A. V. Burenin, "Theoretical analysis of the gas cell of a microwave spectroscopy with an acoustic detector," *Radiophys. Quantum El.*, vol. 17, pp. 984–994, 1974.
- [13] M. Y. Tretyakov, M. A. Koshelev, D. S. Makarov, and M. V. Tonkov, "Precise measurements of collision parameters of spectral lines with a spectrometer with radioacoustic detection of absorption in the millimeter and submillimeter ranges," *Instrum. Exp. Techn.*, vol. 51, pp. 78–88, 2008.
- [14] M. A. Koshelev, G. Y. Golubiatnikov, I. N. Vilkov, and M. Y. Tretyakov, "Line shape parameters of the 22-GHz water line for accurate modeling in atmospheric applications," *J. Quant. Spectrosc. Radiative Transfer*, vol. 205, pp. 51–58, 2018.
- [15] A. F. Krupnov and A. V. Burenin, "On the theory of microwave spectrometers," *Izv. VUZov. Radiofizika*, vol. 22, no. 3, pp. 305–313, 1979.
- [16] A. V. Burenin and A. F. Krupnov, "Possibility of observing the rotational spectra of nonpolar molecules," *JETP*, vol. 40, pp. 252–253, 1975.
- [17] V. S. Letokhov and V. P. Chebotayev, *Nonlinear Laser Spectroscopy of High Resolution*. Moscow, Russia: Nauka, 1990.
- [18] A. M. Kiselev, Y. N. Ponomarev, A. N. Stepanov, A. B. Tikhomirov, and B. A. Tikhomirov, "Absorption of a femtosecond Ti:Sa-laser radiation by atmospheric air and water vapor," *Atmospheric Ocean. Opt.*, vol. 19, pp. 608–613, 2006.
- [19] V. S. Kozlov, M. V. Panchenko, A. B. Tikhomirov, and B. A. Tikhomirov, "Measurement of aerosol absorption of radiation with a wavelength of 694.300 nm in the surface layer of air," *Atmospheric Ocean. Opt.*, vol. 15, pp. 756–761, 2002.
- [20] L. A. Surin, B. S. Dumesh, F. S. Rusin, G. Winnewisser, and I. Pak, "Doppler-free two-photon millimeter wave transitions in OCS and CHF<sub>3</sub>," *Phys Rev. Lett.*, vol. 86, no. 10, pp. 2002–2005, 2001.
- [21] O. I. Permyakova, E. Ilisca, and P. L. Chapovsky, "Theoretical model for enrichment of CH<sub>3</sub>F nuclear-spin isomers by resonant microwave radiation," *Phys. Rev. A*, vol. 67, 2003, Art. no. 033406.
- [22] A. Miyazaki *et al.*, "First millimeter-wave spectroscopy of ground-state positronium," *Prog. Theor. Exp. Phys.*, vol. 2015, 2015, Art. no. 011C01, doi: [10.1093/ptep/ptu181](https://doi.org/10.1093/ptep/ptu181).
- [23] I. I. Antakov *et al.*, "Use of large powers of resonant radiation for enhancing the sensitivity of microwave spectrometers," *JETP Lett.*, vol. 19, pp. 634–637, 1974.
- [24] M. Y. Glyavin *et al.*, "High power terahertz sources for spectroscopy and material diagnostics," *Phys. Usp.*, vol. 59, no. 6, pp. 595–604, 2016.
- [25] M. Thumm, "State-of-the-art of high-power gyro-devices and free electron masers," *Int. J. IR MM Waves*, vol. 41, pp. 1–140, 2020, doi: [10.1007/s10762-019-00631-y](https://doi.org/10.1007/s10762-019-00631-y).
- [26] M. A. Koshelev, A. I. Tsvetkov, M. V. Morozkin, M. Y. Glyavin, and M. Y. Tretyakov, "Molecular gas spectroscopy using radioacoustic detection and high-power coherent subterahertz radiation sources," *J. Mol. Spectrosc.*, vol. 331, pp. 9–16, 2017.
- [27] M. Y. Glyavin *et al.*, "Experimental tests of 263 GHz gyrotron for spectroscopy applications and diagnostic of various media," *Rev. Sci. Instr.*, vol. 86, no. 5, 2015, Art. no. 054705.
- [28] A. P. Fokin *et al.*, "High-power sub-terahertz source with a record frequency stability at up to 1 Hz," *Sci. Rep.*, vol. 8, 2018, Art. no. 4317.
- [29] B. G. Danly, W. J. Mulligan, R. J. Temkin, and T. C. L. G. Sollner, "Highpower second harmonic emission and frequency locking in a 28 GHz gyrotron," *Appl. Phys. Lett.*, vol. 46, 1985, Art. no. 728.
- [30] S. Alberti *et al.*, "Experimental measurements of competition between fundamental and second harmonic emission in a quasi-optical gyrotron," *Phys. Fluids B: Plasma Phys.*, vol. 2, no. 11, 1990, Art. no. 2544.
- [31] G. S. Nusinovich and A. B. Paveliev, "Theoretical study of spurious generation at the harmonics of the operating-mode frequency in gyrotrons," *Radiotekh. Elektron.*, vol. 32, pp. 1274–1280, 1987.
- [32] N. A. Zavolsky, G. S. Nusinovich, and A. B. Paveliev, "Toward the theory of parasitic radiation in gyrotrons," *Radiophys. Quantum El.*, vol. 31, pp. 269–275, 1988.
- [33] L. I. Gershtein, "Optimal acoustic receiving system for microwave spectrometers with acoustic detection," *Izv. Vyssh. Uchebn. Zaved. Radiofizika*, vol. 20, no. 2, pp. 223–231, 1977.
- [34] W. Demtröder, *Laser Spectroscopy: Basic Concepts and Instrumentation*, 3rd ed. New York, NY, USA: Springer.
- [35] C. H. Townes and A. Schawlow, *Microwave Spectroscopy*. New York, NY, USA: Dover, 1975, pp. 435–441 (unabridged and corrected republication of the work first published in 1955 by the McGraw-Hill).
- [36] E. Klisch, P. Schilke, S. P. Belov, and G. Winnewisser, "<sup>33</sup>SO<sub>2</sub>: Interstellar identification and laboratory measurements," *J. Mol. Spectrosc.*, vol. 186, no. 2, pp. 314–318, 1997.
- [37] S. P. Belov *et al.*, "High frequency transitions in the rotational spectrum of SO<sub>2</sub>," *J. Mol. Spectrosc.*, vol. 191, pp. 17–27, 1998.
- [38] B. Sumpf, M. Schone, O. Fleischmann, Y. Heiner, and H. D. Kronfeldt, "Quantum number and temperature dependence of foreign gas-broadening coefficients in the nu(1) and nu(3) bands of SO<sub>2</sub>: Collisions with H<sub>2</sub>, Air, He, Ne, Ar, Kr, and Xe," *J. Mol. Spectrosc.*, vol. 183, pp. 61–71, 1997.
- [39] I. E. Gordon *et al.*, "The HITRAN2016 molecular spectroscopic database," *J. Quant. Spectrosc. Radiative Transfer*, vol. 203, pp. 3–69, 2017.
- [40] J. Reid and D. Labrie, "Second-harmonic detection with tunable diode lasers—Comparison of experiment and theory," *Appl. Phys. B.*, vol. 26, pp. 203–210, 1981.
- [41] G. Y. Golubiatnikov, S. P. Belov, and A. V. Lapinov, "The features of the frequency-modulation method when studying the shapes of the spectral lines of nonlinear absorption," *Radiophysics Quantum Electron.*, vol. 59, no. 8–9, pp. 715–726, 2017.
- [42] C. Winnewisser, F. Lewen, and H. Helm, "Transmission characteristics of dichroic filters measured by THz time-domain spectroscopy," *Appl. Phys. A*, vol. 66, pp. 593–598, 1998.
- [43] C. Winnewisser, F. T. Lewen, M. Schall, M. Walther, and H. Helm, "Characterization and application of dichroic filters in the 0.1–3-THz region," *IEEE Trans. Microw. Theory Tech.*, vol. 48, no. 4, pp. 744–749, Apr. 2000.
- [44] W. J. Lafferty, *Private Communication*, 1994.
- [45] H. M. Pickett *et al.*, "Submillimeter, millimeter, and microwave spectral line catalog," *J. Quant. Spectrosc. Radiative Transfer*, vol. 60, pp. 883–890, 1998. [Online]. Available: <https://spec.jpl.nasa.gov/ftp/pub/catalog/catform.html>
- [46] G. Y. Golubiatnikov, A. V. Lapinov, A. Guarnieri, and R. Knochel, "Precise lamb-dip measurements of millimeter and submillimeter wave rotational transitions of <sup>16</sup>O<sup>12</sup>C<sup>32</sup>S," *J. Mol. Spectrosc.*, vol. 234, pp. 190–194, 2005.
- [47] A. F. Krupnov *et al.*, "Technique of broadband measurements of frequency conversion efficiency for each harmonique in frequency multipliers up to terahertz range," *Int. J. IR MM Waves*, vol. 21, no. 3, pp. 343–354, 2000.

- [48] M. A. Koshelev, I. N. Vilkov, O. Egorov, A. V. Nikitin, and M. Rey, "High-sensitivity measurements of  $^{12}\text{CH}_3\text{D}$  pure rotational lines in ground and excited vibrational states in the subTHz region," *J. Quant. Spectrosc. Radiative Transfer*, vol. 242, 2020, Art. no. 106781, doi: 10.1016/j.jqsrt.2019.106781.
- [49] I. Ozier, W. Ho, and G. Birnebaum, "Pure rotational spectrum and electric dipole moment of  $\text{CH}_3\text{D}$ ," *J. Chem. Phys.*, vol. 51, no. 11, pp. 4873–4880, 1969.
- [50] V. M. Devi, D. C. Benner, M. A. H. Smith, C. P. Rinsland, and L. R. Brown, "Self- and  $\text{N}_2$ -broadening, pressure induced shift and line mixing in the  $\nu_5$  band of  $^{12}\text{CH}_3\text{D}$  using a multispectrum fitting technique," *J. Quant. Spectrosc. Radiative Transfer*, vol. 74, pp. 1–41, 2002.
- [51] Y. A. Ba *et al.*, "MeCaSDa and ECaSDa: Methane and ethene calculated spectroscopic databases for the virtual atomic and molecular data centre," *J. Quant. Spectrosc. Radiative Transfer*, vol. 130, pp. 62–68, 2013.
- [52] V. Boudon *et al.*, "The high-resolution far-infrared spectrum of methane at the SOLEIL synchrotron," *J. Quant. Spectrosc. Radiative Transfer*, vol. 111, pp. 1117–1129, 2010.
- [53] C. Bray *et al.*, "Spectral lines of methane measured up to 2.6 THz at sub-MHz accuracy with a CW-THz photomixing spectrometer: Line positions of rotational transitions induced by centrifugal distortion," *J. Quant. Spectrosc. Radiative Transfer*, vol. 203, pp. 349–354, 2017.
- [54] Y. Endo and M. Mizushima, "Microwave resonance lines of  $^{16}\text{O}_2$  in its electronic ground state ( $X^3\Sigma_g^-$ )," *Jpn. J. Appl. Phys.*, vol. 21, 1982, Art. no. L379.
- [55] T. Amano and E. Hirota, "Microwave spectrum of the molecular oxygen in the excited vibrational state," *J. Mol. Spec.*, vol. 53, pp. 346–363, 1974.
- [56] Y. Endo, K. Yoshida, S. Saito, and E. Horota, "The microwave spectrum of carbon dioxide— $^{18}\text{O}$ ," *J. Chem. Phys.*, vol. 73, 1980, Art. no. 3511.
- [57] J. Gripp, H. Mäder, H. Dreizler, and J. L. Teffo, "The microwave spectrum of carbon dioxide  $^{17}\text{OCO}$  and  $^{18}\text{OCO}$ ," *J. Mol. Spectr.*, vol. 172, pp. 430–434, 1995.
- [58] H. Kanamori, Z. T. Dehghani, A. Mizoguchi, and Y. Endo, "Detection of microwave transitions between ortho and para states in a free isolated molecule," *Phys. Rev. Lett.*, vol. 119, 2017, Art. no. 173401.



**German Yu. Golubiatnikov** received the B.S. and M.S. degrees in radiophysics from N.I. Lobachevsky State University of Nizhny Novgorod, Nizhny Novgorod, Russia and the Ph.D. degree in plasma physics from the Institute of Applied Physics of the Russian Academy of Sciences (IAP RAS), Nizhny Novgorod, Russia, in 1996.

Since 1983 he is with the IAP RAS. His scientific interests are mostly connected with the new technique of sub-millimeter microwave spectroscopy, and the application of sub-millimeter-wave systems for technology, as well as the spectroscopy of biosystems.



**Maksim A. Koshelev** graduated from the Radio Physical Faculty of Nizhny Novgorod State University, Nizhny Novgorod, Russia, in 2003 with B.S. and M.S. degrees in radiophysics. He received the Ph.D. degree in physics from the Institute of Applied Physics of the Russian Academy of Sciences (IAP RAS), Nizhny Novgorod, Russia, in 2007.

Since 2000 he is with the Microwave Spectroscopy Lab of IAP RAS. His scientific interests are in the field of experimental molecular spectroscopy, including development of methods and technique, line shape

analysis, and continuum absorption study.



**Alexander I. Tsvetkov** received the M.S. degree in radiophysics from the Lobachevsky State University of Nizhny Novgorod, Nizhny Novgorod, Russia, in 2008, and the Ph.D. degree in engineering from Nizhny Novgorod State Technical University R.E. Alekseev, Nizhny Novgorod, Russia, in 2011.

He is with the Laboratory of Sources and Applications of High-power Terahertz Radiation, Institute of Applied Physics of the Russian Academy of Sciences (IAP RAS), Nizhny Novgorod, Russia.

His main research interests include development of high-frequency, powerful sources of microwave radiation, in particular gyrotrons for spectroscopy and diagnostics of various media.



**Andrei P. Fokin** received the B.S. and M.S. degrees in physics from the Lobachevsky State University of Nizhny Novgorod, Nizhny Novgorod, Russia, in 2014 and the Ph.D. degree in radiophysics from the Institute of Applied Physics of the Russian Academy of Sciences (IAP RAS), Nizhny Novgorod, Russia, in 2018.

Since 2014 he was Junior Researcher and Researcher with the Electronic Devices Department of the Institute of Applied Physics of the Russian Academy of Sciences. He is a Co-Author of more than 30 articles. His research interests include high-frequency gyrotrons, frequency locking and stabilization, microwave spectroscopy, and plasma physics.



**Mikhail Yu. Glyavin** graduated from the Politechnical Institute, Gorky, Russia. He received the Ph.D. degree and Dr.Sci. in physics from the Institute of Applied Physics of the Russian Academy of Sciences (IAP RAS), Nizhny Novgorod, Russia, in 1999 and 2009, respectively. His dissertations were focused on studies of gyrotrons, development of gyrotron-based systems for technological applications and more specifically on methods for increasing the gyrotron efficiency and mastering of THz band.

From 1988 he has been working with IAP RAS where he is developing gyrodevices. Since 1999, at intervals, he was a Visiting Professor with FIR FU Center, Fukui, Japan. Currently he is a Deputy Director in Science and a Head of the Gyrotron Department of IAP RAS. He is a Co-Author of about 200 journal papers. His research interests are in the field of the theoretical and experimental investigations of gyrotrons, and their application to plasma heating, materials processing, and diagnostic of various media.



**Mikhail Yu. Tretyakov** graduated from Gorky State University, Gorky, Russia, in 1980 with M.S. degree in radiophysics. He received the Dr.Sc. degree from the Institute of Applied Physics of the Russian Academy of Sciences (IAP RAS), Nizhny Novgorod, Russia, in 2017.

Since 1980 he has been with IAP RAS, where currently he is the Head of the Laboratory of Microwave Spectroscopy. In 2015–2018 he was member of *Journal of Molecular Spectroscopy* editorial board.